Chiral and kryptoracemic Dy(III) complexes with field-induced single molecule magnet behavior

Article (Accepted Version)

Journal Name

ARTICLE

Chiral and kryptoracemic Dy(III) complexes with field-induced single molecule magnet behavior

Received 00th January 20xx,
Accepted 00th January 20xx

DOI: 10.1039/x0xx00000x

www.rsc.org/

Ying-Ying Zhang[a], Jing-Tao Yu[a], Bo Li[b,*] De-Jing Li[c], Zhi-Gang Gu[c], Xiao-Fan Sun[d], Hong-Ling Cai[d], George E. Kostakis[e], Guo Peng[a,*]

Two mononuclear Dy(III) compounds formulated as $[Dy(PNO)_6(H_2O)_2]Br_3$ (**1**) and $[Dy(PNO)_6(NO_3)](ClO_4)_2$ (**2**) have been synthesized and characterized. Single crystal X-ray diffraction studies show that chiral and kryptoracemic strcuctures are formed when different anions are introduced into the system. **1** crystallizes in the non-polar orthorhombic space group $P2_12_12_1$, whereas **2** assembles as a kryptoracemate in the polar monoclinic space group $P2_1$. The optical activity of single crystals of these two compounds was confirmed by circular dichroism (CD) studies. Thermal gravimetric analyses (TGA) revealed that they are stable up to 376 K (**1**) and 428 K (**2**). Differential scanning calorimetry (DSC) measurements demonstrate the absence of structural phase transitions over the investigated temperature range. Magnetic studies show that both compounds are field-induced single molecule magnets (SMMs) with energy barriers of 36 (± 0.8) K for **1** and 32 (± 1.4) K for **2**. Furthermore, the dielectric and ferroelectric properties of compound **2** were also investigated.

Introduction

Single molecule magnets (SMMs) have gained the interest of researchers for over twenty years due to their potential applications in high-density information storage, molecular spintronic devices and quantum computing.[1] SMMs exhibit magnetic bistability of a molecular origin under certain temperature (called blocking temperature).[2] The properties of SMMs strongly rely on large spin ground state and strong magnetic anisotropy. The interactions of these two factors lead to an energy barrier to block the magnetization reversal. The quality of the SMMs is determined by the energy barrier, which impedes the spin reorientation, and the blocking temperature, below of which hysteresis loop appears. High energy barriers and blocking temperatures have been achieved recently by tailoring the ligand field and the symmetry around metal centers, or enhancing the interactions between metal ions.[3] Moreover, these compounds can be considered as multifunctional materials, therefore other properties such as luminescence,[4] conductivity,[5] porosity,[6] chirality[7-8] and ferroelectricity[8-9], are also being explored. The luminescent SMMs provide good opportunities to study the crystal field splittings of lanthanide ions between ground and excited states, establishing correlations between magnetic and luminescent properties.[4] While the combination of magnetic properties and chirality result in fascinating cooperative effects such as magneto-chiral dichroism (MChD)[10] and multiferroicity,[8] which are both useful for developing advanced data storage components.[8] In general, chiral complexes can be constructed from chiral ligands or by spontaneous resolution in the absence of any chiral auxiliary.[11] Several chiral SMMs based on the first method have been reported,[7-8] whereas chiral SMMs obtained by the latter approach are still rare.[12]

Except the fascinating physical properties, another phenomena related to chirality is racemate. A special case of racemic compounds are kryptoracemates (also known as false conglomerates), in which the crystal itself exhibits handedness, despite containing both enantiomers in equal ratio.[13] A survey by Fábián and Brock shows that only 0.1% of organic structures deposited in the Cambridge Structural Database (CSD) are kryptoracemates.[13a] Bernal and Watkins identified only 26 credible kryptoracemates from 1412 chiral metal-organic compounds.[13b] These reports confirm the rarity of kryptoracemates in the literature. Although several compounds have crystallized as kryptoracemate,[14] to the best of our knowledge, only one example of kryptoracemate SMM has been reported before.[8a]

Pyridine-N-oxide (PNO) is a commercial available organic molecule of low cost and along with its derivatives have been used to build SMMs[15]. Taking into account all the above

[a] Herbert Gleiter Institute of Nanoscience, School of Materials Science and Engineering, Nanjing University of Science and Technology, 210094 Nanjing, P. R. China. Email: guopeng@njust.edu.cn
[b] College of Chemistry and Pharmaceutical Engineering, Nanyang Normal University, Nanyang 473061, P. R. China. Email: libozzu0107@163.com
[c] State Key Laboratory of Structural Chemistry, Fujian Institute of Research on the S tructure of Matter, Chinese Academy of Sciences, 350002 Fuzhou, P. R. China.
[d] Collaborative Innovation Center of Advanced Microstructures, Lab of Solid State Microstructures, School of Physics, Nanjing University, Nanjing 210093, P. R. Chin a.
[e] Department of Chemistry, School of Life Sciences, University of Sussex, Brighton, BN1 9QJ, UK.

Electronic Supplementary Information (ESI) available: Spectra, PXRD patterns, TGA and DSC curves, additional magnetic data, tables, dielectric and ferroelectric plots. CCDC 1817873 and 1817874. See DOI: 10.1039/x0xx00000x

consideration, we present herein the syntheses and structural determination of two mononuclear Dy(III) SMMs formulated as $[Dy(PNO)_6(H_2O)_2]Br_3$ (**1**) and $[Dy(PNO)_6(NO_3)](ClO_4)_2$ (**2**). The use of different anions leads to the formation of chiral and kryptoracemic structures. The circular dichroism (CD), thermal stability, differential scanning calorimetry (DSC) analysis, and magnetic, dielectric and ferroelectric properties of these two compounds have also been investigated.

Experimental section

General Materials and Methods

All the chemicals were obtained from commercial sources, and were used as received without further purification. All reactions were performed under aerobic condition. Elemental analyses (C, H, and N) were carried out on a Vario MICRO cube elemental analyzer. Fourier transform infrared (IR) spectra were measured on a Nicolet IS10 Spectrum with samples prepared as KBr discs. The solid-state circular dichroism (CD) spectra were recorded on a Bio-logic MOS-450 CD Spectrometer with KBr pellets. Powder X-Ray diffraction (PXRD) patterns for both complexes were measured at room temperature using a Bruker D8 ADVANCE X-ray diffractometer. Thermal gravimetric analyses (TGA) were conducted on a Mettler-Toledo TGA/SDTA851 thermoanalyzer at a heating rate of 10K/min under nitrogen atmosphere. Differential scanning calorimetry (DSC) curves were recorded on a Mettler-Toledo DSC 1 instrument at a heating rate of 5K/min under nitrogen atmosphere. Direct current (dc) magnetic measurements were performed on a Quantum Design PPMS DynaCool-9 magnetometer and altering current (ac) magnetic measurements were carried out on a Quantum Design MPMS3 magnetometer. The magnetic data were corrected for diamagnetic contribution by using Pascal's constants. Dielectric permittivities were measured using a Tonghui TH2828A LCR meter. The *P-E* hysteresis loops measurements were recorded on a Precision Premier II Ferroelectric Tester.

Caution! The Dysprosium salt $Dy(ClO_4)_3{\cdot}6H_2O$ using in this study is potentially explosive and should be handled carefully.

Synthetic procedures of compounds 1 and 2

Synthesis of $[Dy(PNO)_6(H_2O)_2]Br_3$ (**1**)

A mixture of pyridine-N-oxide (0.333g, 3.5mmol) and $DyBr_3{\cdot}6H_2O$ (0.255g, 0.5mmol) in CH_3CN (15mL) was sealed in a 25mL Teflon reactor. The reaction mixture was kept at 120°C for 72 h and then cooled to room temperature at a rate of 5°C /h. After cooling, the resulting mixture was filtered. The filtrate was kept in refrigerator (4-8°C) and crystals were obtained after several days. Yield: 206mg (41% based on Dy). Calc. (%) for $C_{30}H_{34}Br_3DyN_6O_8{\cdot}H_2O$: C 35.09, H 3.53, N 8.18; found: C 35.06, H 3.37, N 8.14. Selected IR data (cm^{-1}): 3273(br), 3115(w), 3049(w), 1628(w), 1471(s), 1330(w), 1223(s), 1179(w), 1168(w), 1072(w), 1022(w), 924(w), 839(m), 779(m), 679(w), 560(w), 465(w) (Fig. S1a).

Synthesis of $[Dy(PNO)_6(NO_3)](ClO_4)_2$ (**2**)

Pyridine-N-oxide (0.333g, 3.5mmol), $Dy(ClO_4)_3{\cdot}6H_2O$ (0.170g, 0.3mmol) and $Dy(NO_3)_3{\cdot}6H_2O$ (0.091g, 0.2mmol) was dissolved in C_2H_5OH (22mL). The resulting mixture was heated at 55°C for 3h and then filtered when the solution was cooled. The filtrate was kept in refrigerator (4-8°C) and crystals were obtained after several days. Yield: 102mg (21% based on Dy). Calc. (%) for $C_{30}H_{30}Cl_2DyN_7O_{17}$: C 36.25, H 3.04; N 9.86; found: C 36.28, H 3.02, N 9.88. Selected IR data (cm^{-1}): 3432(br), 3119(w), 1611(w), 1472(s), 1384(w), 1293(w), 1225(m), 1178(w), 1088(m), 1022(w), 841(w), 772(w), 674(w), 624(w), 562(w), 464(w) (Fig. S1b).

Single crystal X-ray diffraction

The crystallographic data of **1** and **2** were collected on a Bruker SMART APEX II diffractometer using monochromated Mo-Kα radiation (λ=0.71073Å) at 173(2) K (**1**) and 166(2) K (**2**). The sorption corrections were performed for both compounds using SADABS supplied by Bruker. Both structures were solved by direct methods and refined by full-matrix least squares analysis on F^2, using the SHELXTL program package[16]. The crystal structure of **2** was refined as a two-component inversion twin. Two perchlorate anions in **2** were found to be disordered. Attempts to refine the structure of **2** in the achiral $P2_1/c$ space group gave unreasonable results. In order to confirm the space group of **2** and exclude phase transitions, the crystallographic data of **2** were also recorded at 218 K and 296 K. Both the crystal structures of **2** at 218 K and 296 K could be refined in the $P2_1/c$ space group (**2a** and **2b,** ESI) with serious disorder of the PNO ligand. Though it seems that the data at 218K and 296K could be both refined in space group $P2_1/c$ from the crystallographic point of view, the crystals of **2** show optical activity confirmed by CD spectra at room temperature (see 'CD spectra' section below) and DSC measurements below room temperature (see 'PXRD, TGA and DSC characterizations' section below) indicate no structural phase transitions, which is contradictory with the crystallographic data at 218 K and 296 K. Therefore, the space group of **2** below room temperature was determined as $P2_1$ rather than $P2_1/c$. Ordered non-H atoms were refined anisotropically, H-atoms were placed in calculated positions and refined using a riding model. Details of the crystal structures, data collection and refinement are summarized in Table 1.

Results and discussions

Synthetic aspects

The reactions of PNO and dysprosium salts ($DyBr_3{\cdot}6H_2O$ / mixture of $Dy(ClO_4)_3{\cdot}6H_2O$ and $Dy(NO_3)_3{\cdot}6H_2O$) in the ratio of 7:1 in CH_3CN / C_2H_5OH produce crystals **1** and **2**. The replacement of $DyBr_3{\cdot}6H_2O$ by $DyCl_3{\cdot}6H_2O$ yielded complex $[Dy(PNO)_6(H_2O)_2]Cl_3$ (**3**) which is isoskeletal with **1**, and the results have been published by some of us.[12b] Although one kryptoracemic complex $[Eu(PNO)_8](ClO_4)_3$ (**4**) have been reported before,[17] the preparation of its Dy analogue was

Table 1 Crystallographic data and structure refinement for compounds **1** and **2**

	1	**2**
Formula	$C_{30}H_{34}Br_3DyN_6O_8$	$C_{30}H_{30}Cl_2DyN_7O_{17}$
M_r (g mol^{-1})	1008.86	994.01
Crystal system	Orthorhombic	Monoclinic
Space group	$P2_12_12_1$	$P2_1$
T (K)	173(2)	166(2)
a (Å)	9.6000(4)	18.0243(8)
b (Å)	9.8600(4)	10.3625(4)
c (Å)	37.7277(17)	20.7752(9)
α (º)	90	90
β (º)	90	107.417(2)
γ (º)	90	90
V (Å^3)	3571.2(3)	3702.4(3)
Z	4	4
D_c (g cm^{-3})	1.876	1.783
μ (mm^{-1})	5.505	2.248
F(000)	1964	1980
Reflns collected	36031	22267
Unique reflns	6544	11350
R_{int}	0.0879	0.0605
GOF	1.085	1.033
R_1(I > 2σ)	0.0451	0.0409
wR_2 (all data)	0.0534	0.0535
Max. diff. peak / hole (e Å^{-3})	0.950/ -0.984	0.53/ -0.49
Flack parameter	0.002(10)	0.414(15)
CCDC	1817873	1817874

unsuccessful by only introducing $Dy(ClO_4)_3{\cdot}6H_2O$ into the system, even when we increased the PNO/$Dy(ClO_4)_3{\cdot}6H_2O$ ratios from 7:1 to 16:1 (Table S1). This differentiation may be attributed to the relatively smaller radius of Dy ion that disfavors coordination to eight PNO ligands. When other Dy salts, such as $Dy(NO_3)_3{\cdot}6H_2O$, $Dy(OAc)_3{\cdot}4H_2O$ or $Dy(OTf)_3$, were employed in the given reaction in place of $DyBr_3{\cdot}6H_2O$ or $DyCl_3{\cdot}6H_2O$, non-crystalline materials were obtained. Therefore, we decided to explore the mixed Dy salts synthetic strategy to obtain other crystalline products. Compound **2** was obtained from the reaction of PNO, $Dy(NO_3)_3{\cdot}6H_2O$ and $Dy(ClO_4)_3{\cdot}6H_2O$ in the ratio of 35:2:3. Changing the ratio from 35:2:3 to 21:1:2 yielded the same product, in lower yields, as it was demostrated by IR and PXRD studies. It is worth noting that $DyBr_3{\cdot}6H_2O$ has poor solubility in CH_3CN therefore the reaction that yields **1** takes place under solvothermal conditions (120°C for 72 h) to increase its solubility, whereas the reaction that yields **2** incorporates a protic solvent (EtOH) in which the metal salts are more soluble and thus requires lower temperature conditions (55°C for 3h). This reaction is phase pure and reproducible as it is confirmed by PXRD studies (see 'PXRD, TGA and DSC characterizations' section below). No other crystalline products were obtained when other mixtures of Dy salts and solvents were incorporated in the given reaction (Table S1). The crystals of **1** and **2** are sensitive to moisture and thus should be conserved in drying cabinet.

Structural description

The molecular structures of **1** and **2** were established by single crystal X-ray diffraction and depicted in Fig. 1. Complex **1** crystallizes in the non-polar orthorhombic space group $P2_12_12_1$, while complex **2** assembles as a kryptoracemate in the polar monoclinic space group $P2_1$. Each asymmetric unit of **1** consists of one Dy(III) ion, six PNO ligands, two coordinated water molecules and three lattice Br^- anions. The Dy(III) ion coordinate to six PNO ligands and two coordinated water molecules, resulting in a triangular dodecahedral coordination geometry (D_{2d} symmetry), which is confirmed by continuous shape measures (Table S2).[18] The Dy-O band distances vary from 2.320(4) to 2.420(4). For complex **2**, there are two oppositely handed stereoisomers $[Dy(PNO)_6(NO_3)]^{2+}$ and four ClO_4^- in the asymmetric unit. Both Dy(III) ions are coordinated by eight oxygen donors from six PNO ligands and one NO_3^- group with the Dy-O bond distances fall in the range of 2.260(13)-2.511(12) Å. The coordination geometry around Dy1 ion can be described as square antiprism (D_{4d} symmetry),

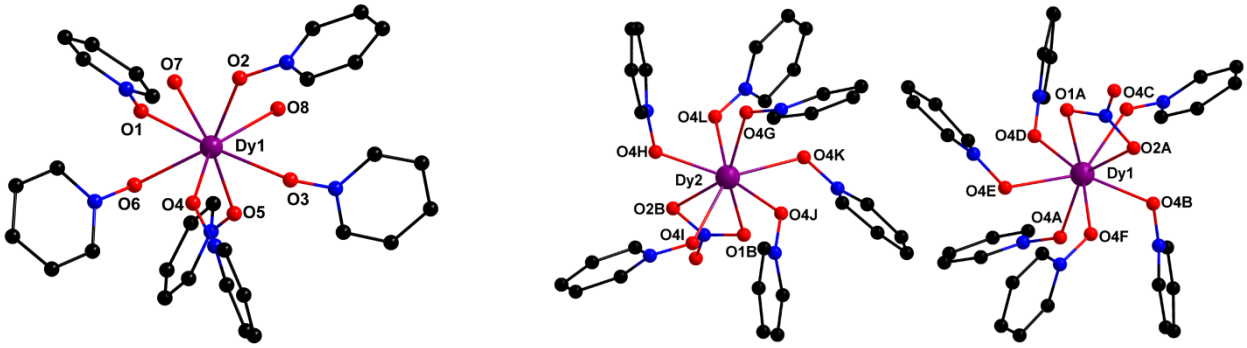

(a) **(b)**

Fig. 1 Molecular structures of complexes **1** (a) and **2** (b). Dy, O, N and C are shown in violet, red, blue and black, respectively. H atoms and lattice anions are omitted for clarity.

whereas the coordination geometry of Dy2 is between square antiprism and biaugmented trigonal prism (C_{2v} symmetry) establishing by continuous shape measures program (Table S2).[18] The shortest distance between neighboring Dy(III) ions is 9.6000(6) Å for **1** and 10.0676(11) for **2**, respectivly, suggesting well seperation between different Dy(III) monomers.

CD spectra

The solid-state circular dichroism (CD) spectra of **1** and **2** were recorded on single crystals with KBr pellets at room temperature. Opposite Cotton effects were observed at 292nm for crystals of **1**, and at 254nm for crystals of **2** (Fig. 2), indicating the formation of enantiomers in the process of spontaneous resolution. The mirror imaged CD spectra of **1** and **2** confirmed optical activities of their crystals.

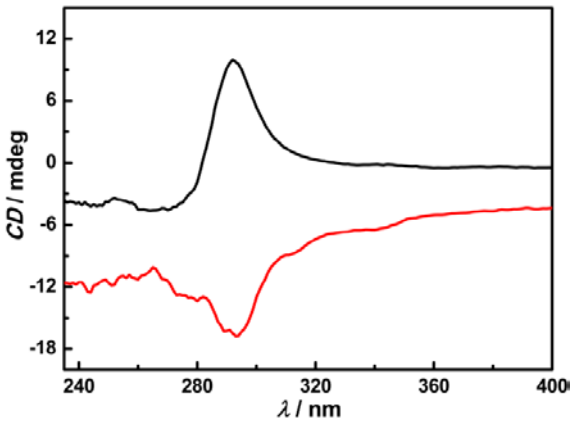

(a)

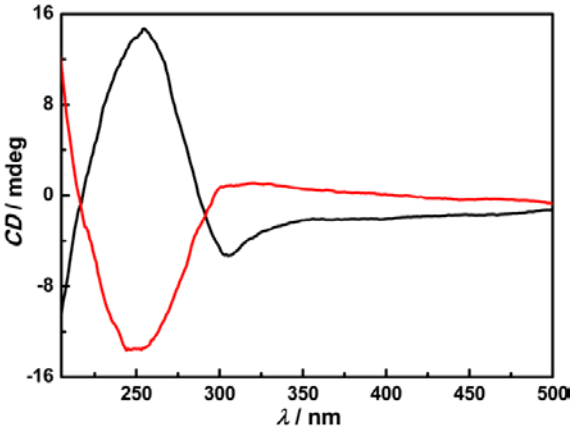

(b)

Fig. 2 Solid-state CD spectra of complexes **1** (a) and **2** (b) at room temperature.

To further explore the enantiomeric excess in these complexes, the CD spectra for bulk samples of **1** and **2** were recorded. In each case, a silent CD spectrum for **1** and **2** is obtained (Fig. S2), suggesting that the resulting crystals are racemic mixtures. To the best of our knowledge, only two kryptoracemic compounds showing CD signals have been reported before.[8a, 14a]

PXRD, TGA and DSC characterizations

Powder X-ray diffraction (PXRD) measurements were conducted on complexes **1** and **2** to check the purity of the bulk sample. As shown in Fig. S3, the experimental PXRD patterns of both products match well with that from simulation based on single crystal diffraction, demonstrating the pure phase of both complexes. The thermal stability of complexes **1** and **2** were examined by thermal gravimetric analysis (TGA) technique under N_2. The results show that they are stable up to 376K for **1** and 428K for **2** (Fig. S4), above which decomposition starts. No weight loss was detected before collapse, suggesting the absence of solvent molecules in the lattice. The differential scanning calorimetry (DSC) analysis show that there are no structural phase transitions were observed from 123-361K for **1** and 123-413K for **2** (Fig. S5). This behavior indicates that the structures of both complexes maintain crystallizing in chiral space group over the investigated temperature range.

Magnetic properties

Magnetic susceptibility measurements for polycrystalline samples of **1** and **2** were performed under 1000Oe applied field in the temperature range of 2-300K. The χT values at 300 K are 14.08 cm^3 K mol^{-1} for **1** and 14.02 cm^3 K mol^{-1} for **2**, both are close to the value 14.17 cm^3 K mol^{-1} expected for one isolated Dy(III) ion (Fig. 3). With cooling, the χT values steadily decrease to 10.81 cm^3 K mol^{-1} for **1** and 9.28 cm^3 K mol^{-1} for **2** at 2 K, which could be due to the thermal depopulation of the m_J sublevels of Dy(III) centers. The field dependence of the magnetization below 5K increase gradually with rising applied field and reach 5.49 Nβ for **1** and 5.55 Nβ for **2** at 2K and 7T (Fig. S6). These values are much lower than that of saturation (10 Nβ) for one Dy(III) ion, indicating the presence of magnetic anisotropy and/or low lying-excited states in both complexes. The M versus HT^{-1} plots below 5K are non-overlapping (Fig. S7), which further confirms the existence of such effects.

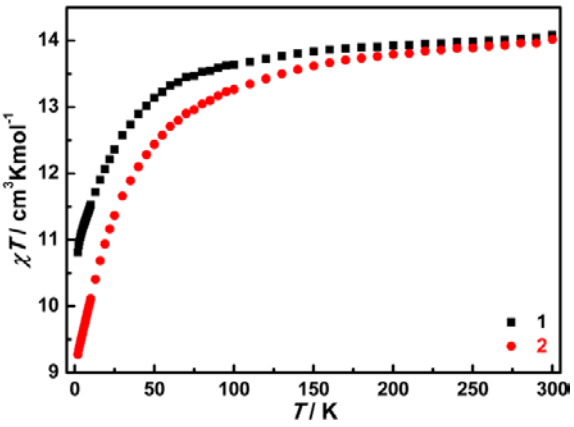

Fig. 3 Temperature dependence of the χT products of complexes **1** and **2**.

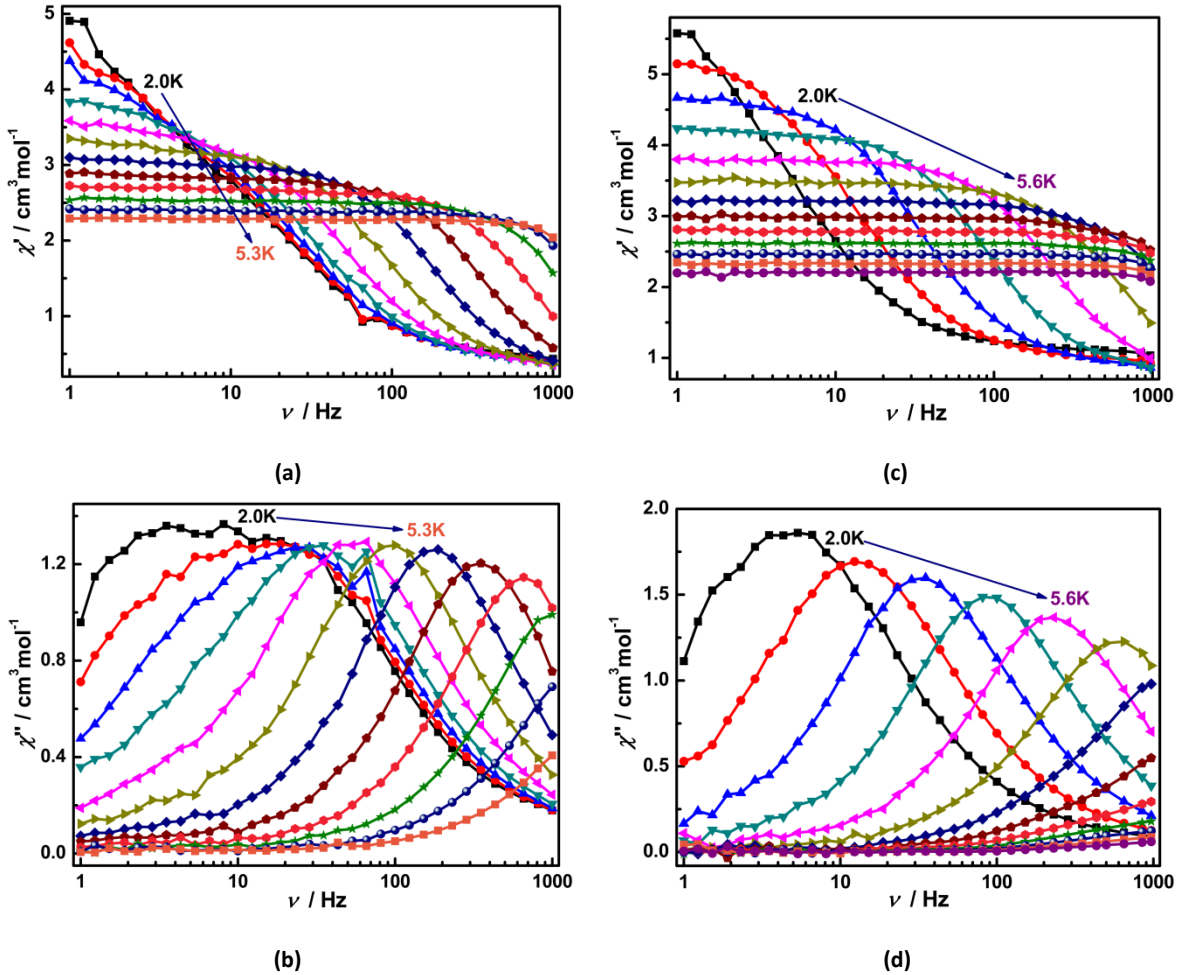

Fig. 4 Frequency dependence of in-phase and out-of-phase ac susceptibility signals under 1200 Oe and 500 Oe dc field for complexes **1** (a, b) and **2** (c, d).

Alternating current (ac) susceptibility measurements were conducted to investigate the magnetic dynamic of these two complexes. No out-of-phase signals were detected in the absence of dc field, which is probably due to fast quantum tunneling of magnetization (QTM). Generally, the QTM can be suppressed by the application of an external dc field. Therefore, further ac susceptibility measurements were conducted under various dc fields at 2 K (Fig S8 and Fig S9). Well-defined maxima were observed in out-of-phase components by the application of dc field varying from 200 to 2500 Oe, suggesting the suppression of QTM. As shown in Fig S10, the relaxation is minimized at 1200 and 500 Oe for **1** and **2**. Therefore, the frequency dependence of ac susceptibility at different temperatures was measured at these optimum fields. This results in strong out-of-phase ac signals with clear peaks (Fig. 4), indicating field-induced SMM behavior of **1** and **2**. The Cole-Cole plots of **1** and **2** can be fitted by a generalized Debye model (Fig.

S11),[19] resulting in α = 0.008-0.37 for **1** and 0.06-0.22 for **2** (Table S3 and Table S4), which indicate a medium distribution of the relaxation time. The Arrhenius curves can be established by results from the Cole-Cole plots fitting. By only considering the Orbach process, a tentative fit to the high temperature data gave the following results: U_{eff} = 36 (± 0.8) K with τ_0 = 6.6 (± 1.2) × 10^{-8} s for **1**, and U_{eff} = 32 (± 1.4) K with τ_0 = 3.3 (± 1.3) × 10^{-8} s for **2** (Fig. 5). To further study the relaxation mechanism of these two complexes, the Lnτ versus LnT curves were plotted. The linear fittings to $\tau \sim T^{-n}$ result in n = 8.16 for **1** and 8.78 for **2** (Fig. S12), which are close to n = 9 for a Kramers ion,[20] suggesting the presence of Raman process in these two complexes. No best-fitting result can be obtained by only considering Raman process for **1**. Further considering both the Raman and QTM processes ($\boldsymbol{\tau^{-1} = CT^n + \tau_{QTM}^{-1}}$), the fitting of τ versus T plot lead to satisfied results with C = 0.014 s^{-1} $K^{-8.46}$, n = 8.46, $\boldsymbol{\tau_{QTM}^{-1}}$ = 60 s^{-1}, confirming the magnetic relaxation of **1** is realized by the mixture of Raman and QTM processes (Fig. 5). This model has also been employed before by Colacio.[21] In contrast, the τ versus T curves of **2** can be fitted well by considering only Raman processes ($\boldsymbol{\tau^{-1} = CT^n}$) with n fixing to be 8.78 and C = 0.057 s^{-1} $K^{-8.78}$, verifying the magnetic relaxation of **2** is dominated by Raman processes (Fig. 5). Magnetic hysteresis measurements were carried out on both complexes at 2 K with a field weep rate of 200 Oe/s, but no hysteresis loops were observed (Fig. S13). This observation indicates fast relaxation of magnetization in these two complexes. Different magnetic relaxation behaviors observed in **1** and **2** can be ascribed to the dissimilar coordination environments of Dy(III) ions. It is well established that the dynamic magnetic behavior of SMMs is sensitive to the subtle changes in ligand field and/or local geometric symmetry around metal centers. The replacement of two coordinated water molecules in **1** by one NO_3^- group in **2** leads to distinct ligand fields and symmetries around Dy(III) ions, which may significantly affect the magnetic anisotropy, resulting in different relaxation behaviors.

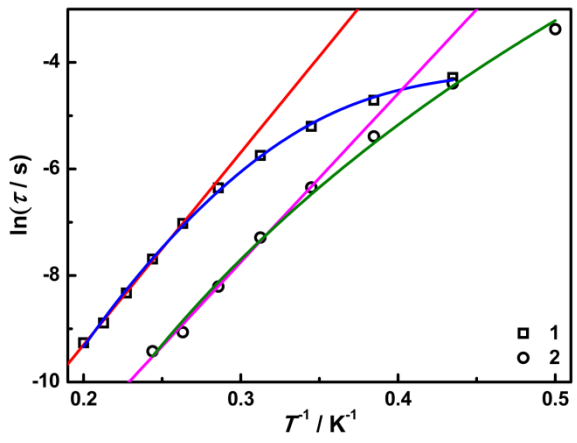

Fig. 5 Temperature dependence of the relaxation times under 1200 and 500Oe dc fields for complexes **1** and **2**. The red and pink lines are the best fits to an Arrhenius law. The blue line is fit for Raman plus QTM processes. The green line is fit for Raman process.

Dielectric and Ferroelectric studies

Compound **2** crystallizes in the polar $P2_1$ space group, therefore dielectric measurements, on a single crystal sample, to determine the polarity of the product were carried out. The dielectric constant increase with heating and reach a value of about 11 at room temperature (Fig. S14), which is in good agreement with that of other molecular ferroelectrics.[22] No anomaly was observed in the dielectric susceptibility from 123-408K, confirming that no phase transitions occur over the investigated temperature range, which is in agreement with the results from DSC measurements. To examine the ferroelectric behavior of complex **2**, polarization measurements as a function of applied electric field were conducted on single crystals at various temperatures. However, no hysteresis was detected even at low temperature (Fig. S15), suggesting weak polarization of the as-synthesized products.

Conclusions

Two mononuclear Dy(III) complexes with diverse polarity have been synthesized and characterized. Complex **1** assembles in the non-polar orthorhombic space group $P2_12_12_1$, while complex **2** crystallizes as a kryptoracemate in the polar monoclinic space group $P2_1$. The structural differences of these two complexes highlight the effect of anions on their framework construction. Magnetic measurements reveal that both complexes display field-induced SMM behavior with energy barriers of 36 (± 0.8) K and 32 (± 1.4) K. Different magnetic relaxation behaviors observed in these two complexes can be attributed to the distinct coordination environments around Dy(III) ions. These two complexes present rare examples of chiral and kryptoracemate SMMs obtained by spontaneous resolution.[13] This work offers an effective way to tune the crystalline modes (chiral for **1** and kryptoracemate for **2**) and manipulate the magnetic relaxation of SMMs.

Conflicts of interest

There are no conflicts to declare

Acknowledgements

This work was supported by the National Natural Science Foundation of China (21501093) and the Natural Science Foundation of Jiangsu Province (BK20150768). BL and ZGG thanks for the financial support from NSFC of China (21401112 and 21601189).

Notes and references

1 (*a*) F. Troiania, M. Affronte, *Chem. Soc. Rev.*, 2011, **40**, 3119; (*b*) L. Bogani, W. Wernsdorfer, *Nat. Mater.*, 2008, **7**, 179; (*c*) M. N. Leuenberger, D. Loss, *Nature*, 2001, **414**, 789.

2 (*a*) S. G. McAdams, A. M. Ariciu, A. K. Kostopoulos, J. P. S. Walsh, F. Tuna, *Coord. Chem. Rev.*, 2017, **346**, 216; (*b*) D. N. Woodruff, R. E. P. Winpenny, R. A. Layfield, *Chem. Rev.*, 2013, **113**, 5110; (*c*) P. Zhang, Y. N. Guo, J. Tang, *Coord. Chem. Rev.*,

2013, **257**, 1728; (*d*) J. L. Liu, Y. C. Chen, M. L. Tong, *Chem. Soc. Rev.*, 2018, **47**, 2431; (*e*) M. Feng, M. L. Tong, *Chem. Eur. J.*, 2018, **24**, 7574.

3 (*a*) C. A. P. Goodwin, F. Ortu, D. Reta, N. F. Chilton, D. P. Mills, *Nature*, 2017, **548**, 439; (*b*) F. S. Guo, B. M. Day, Y. C. Chen, M. L. Tong, A. Mansikkamaki, R. A. Layfield, *Angew. Chem. Int. Ed.*, 2017, **56**, 11445; (*c*) Y. S. Ding, N. F. Chilton, R. E. P. Winpenny, Y. Z. Zheng, *Angew. Chem. Int. Ed.*, 2016, **55**, 16071; (*d*) J. Liu, Y. C. Chen, J. L. Liu, V. Vieru, L. Ungur, J. H. Jia, F. Chibotaru, Y. Lan, W. Wernsdorfer, S. Gao, X. M. Chen, M. L. Tong, *J. Am. Chem. Soc.*, 2016, **138**, 5441; (*e*) Y. C. Chen, J. L. Liu, L. Ungur, J. Liu, Q. W. Li, L. F. Wang, Z. P. Ni, F. Chibotaru, X. M. Chen, M. L. Tong, *J. Am. Chem. Soc.*, 2016, **138**, 2829; (*f*) T. Pugh, N. F, Chilton, R. A. Layfield, *Angew. Chem. Int. Ed.*, 2016, **55**, 11082; (*g*) S. K. Gupta, T. Rajeshkumar, G. Rajaraman, R. Murugavel, *Chem. Sci.*, 2016, **7**, 5181; (*h*) X. N. Yao, J. Z. Du, Y. Q. Zhang, X. B. Leng, M. W. Yang, S. D. Jiang, Z. X. Wang, Z. W. Ouyang, L. Deng, B. W. Wang, S. Gao, *J. Am. Chem. Soc.*, 2017, **139**, 373; (*i*) J. M. Zadrozny, D. J. Xiao, M. Atanasov, G. J. Long, F. Grandjean, F. Neese, J. R. Long, *Nat. Chem.*, 2013, **5**, 577; (*j*) C. R. Ganivet, B. Ballesteros, G. de la Torre, J. M. Clemente-Juan, E. Coronado, T. Torres, *Chem. Eur. J.*, 2013, **19**, 1457; (*k*) J. D. Rinehart, M. Fang, W. J. Evans, J. R. Long, *J. Am. Chem. Soc.*, 2011, **133**, 14236.

4 (*a*) J. H. Jia, Q. W. Li, Y. C. Chen, J. L. Liu, M. L. Tong, *Coord. Chem. Rev.*, 2018, DOI: 10.1016/j.ccr.2017.11.012; (*b*) Y. Bi, C. Chen, Y. F. Zhao, Y. Q. Zhang, S. D. Jiang, B. W. Wang, J. B. Han, J. L. Sun, Z. Q. Bian, Z. M. Wang, S. Gao, *Chem. Sci.*, 2016, **7**, 5020; (*c*) S. Chorazy, M. Rams, K. Nakabayashi, B. Sieklucka, S. Ohkoshi, *Chem. Eur. J.,* 2016, **22**, 7371; (*d*) M. Gregson, N. F. Chilton, A. M. Ariciu, F. Tuna, I. F. Crowe, W. Lewis, A. J. Blake, D. Collison, E. J. L. McInnes, R. E. P. Winpenny, S. T. Liddle, *Chem. Sci.*, 2016, **7**, 155; (*e*) G. Cucinotta, M. Perfetti, J. Luzon, M. Etienne, P. E. Car, A. Caneschi, G. Calvez, K. Bernot, R. Sessoli, *Angew. Chem. Int. Ed.*, 2012, **51**, 1606; (*f*) J. Long, R. Vallat, R. A. S. Ferreira, L. D. Carlos, F. A. A. Paz, Y. Guaria, J. Larionova, *Chem. Commun.*, 2012, **48**, 9974; (*g*) X. Yi, K. Bernot, F. Pointillart, G. Poneti, G. Calvez, C. Daiguebonne, O. Guillou, R. Sessoli, *Chem. Eur. J.,* 2012, **18**, 11379; (*h*) E. L. Gavey, M. A. Hareri, J. Regier, L. D. Carlos, R. A. S. Ferreira, F. S. Razavi, J. M. Rawsond, M. Pilkington, *J. Mater. Chem. C*, 2015, **3**, 7738.

5 X. Zhang, H. Xie, M. Ballesteros-Rivas, T. J. Woods, K. R. Dunbar, *Chem. Eur. J.,* 2017, **23**, 7448.

6 X. Zhang, V. Vieru, X. Feng, J. L. Liu, Z. Zhang, B. Na, W. Shi, B. W. Wang, A. K. Powell, L. F. Chibotaru, S. Gao, P. Cheng, J. R. Long, *Angew. Chem. Int. Ed.*, 2015, **54**, 9861.

7 (*a*) J. K. Ou-Yang, N. Saleh, G. Fernandez Garcia, L. Norel, F. Pointillart, T. Guizouarn, O. Cador, F. Totti, L. Ouahab, J. Crassous, B. Le Guennic, *Chem. Commun.*, 2016, **52**, 14474; (*b*) M. Ren, Z. L. Xu, T. T. Wang, S. S. Bao, Z. H. Zheng, Z. C. Zhang, L. M. Zheng, *Dalton Trans.*, 2016, **45**, 690; (*c*) S. Y. Lin, C. Wang, L. Zhao, J. Wu, J. Tang, *Dalton Trans.*, 2015, **44**, 223; (*d*) M. X. Yao, Q. Zheng, F. Gao, Y. Z. Li, Y. Song, J. L. Zuo, *Dalton Trans.*, 2012, **41**, 13682; (*e*) T. Ueno, T. Fujinami, N. Matsumoto, M. Furusawa, R. Irie, N. Re, T. Kanetomo, T. Ishida, Y. Sunatsuki, *Inorg. Chem.*, 2017, **56**, 1679; (*f*) K. A. Lippert, C. Mukherjee, J. P. Broschinski, Y. Lippert, S. Walleck, A. Stammler, H. Bogge, J. Schnack, T. Glaser, *Inorg. Chem.*, 2017, **56**, 15119; (*g*) H. R. Wen, J. Bao, S. J. Liu, C. M. Liu, C. W. Zhang, Y. Z. Tang, *Dalton Trans.*, 2015, **44**, 11191; (h) A. Escuer, J. Mayans, M. Font-Bardia, L. Di Bari, M. Górecki, *Eur. J. Inorg. Chem.*, 2017, 991.

8 (*a*) X. L. Li, M. Hu, Z. Yin, C. Zhu, C. M. Liu, H. P. Xiao, S. Fang, *Chem. Commun.*, 2017, **53**, 3998; (*b*) J. Long, J. Rouquette, J. M. Thibaud, R. A. S. Ferreira, L. D. Carlos, B. Donnadieu, V. Vieru, L. F. Chibotaru, L. Konczewicz, J. Haines, Y. Guari, J. Larionova, *Angew. Chem. Int. Ed.*, 2015, **54**, 2236; (*c*) X. L. Li, C. L. Chen, Y. L. Gao, C. M. Liu, X. L. Feng, Y. H. Gui, S. M. Fang, *Chem. Eur. J.,* 2012, **18**, 14632; (*d*) J. Liu, X. P. Zhang, T. Wu, B. B. Ma, T. W. Wang, C. H. Li, Y. Z. Li, X. Z. You, *Inorg. Chem.*, 2012, **51**, 8649; (*e*) D. P. Li, T. W. Wang, C. H. Li, D. S. Liu, Y. Z. Li, X. Z. You, *Chem. Commun.*, 2010, **46**, 2929.

9 (*a*) P. H. Guo, Y. Meng, Y. C. Chen, Q. W. Li, B. Y. Wang, J. D. Leng, D. H. Bao, J. H. Jia, *J. Mater. Chem. C*, 2014, **2**, 8858; (*b*) Y. X. Wang, W. Shi, H. Li, Y. Song, L. Fang, Y. Lan, A. K. Powell, W. Wernsdorfer, L. Ungur, L. F. Chibotaru, M. Shen, P. Cheng, *Chem. Sci.*, 2012, **3**, 3366.

10 (*a*) R. Sessoli, M. E. Boulon, A. Caneschi, M. Mannini, L. Poggini, F. Wilhelm, A. Rogalev, *Nat. Phys.*, 2015, **11**, 69; (*b*) C. Train, R. Gheorghe, V. Krstic, L. M. Chamoreau, N. S. Ovanesyan, G. L. J. A. Rikken, M. Gruselle, M. Verdaguer, *Nat. Mater.*, 2008, **7**, 729.

11 B. Q. Song, D. Q. Chen, Z. Ji, J. Tang, X. L. Wang, H. Y. Zang and Z. M. Su, *Chem. Commun.*, 2017, **53**, 1892.

12 (*a*) M. J. Liu, J. Yuan, Y. Q. Zhang, H. L. Sun, C. M. Liu, H. Z. Kou, *Dalton Trans.*, 2017, **46**, 13035; (*b*) G. Peng, Y. Y. Zhang, Z. Y. Li, Inorg. Chem. Commun., 2017, 85, 66; (*c*) P. H. Guo, J. L. Liu, J. H. Jia, J. Wang, F. S. Guo, Y. C. Chen, W. Q. Lin, J. D. Leng, D. H. Bao, X. D. Zhang, J. H. Luo, M. L. Tong, *Chem. Eur. J.*, 2013, **19**, 8769; (*d*) R. Inglis, F. White, S. Piligkos, W. Wernsdorfer, E. K. Brechin, G. S. Papaefstathiou, *Chem. Commun.*, 2011, **47**, 3090.

13 (*a*) L. Fabian, C. P. Brock, *Acta Crystallogr. B*, 2010, **66**, 94; (*b*) I. Bernal, S. Watkins, *Acta Crystallogr. C Struct. Chem.*, 2015, **71**, 216.

14 (*a*) Y. Sunatsuki, K. Fujita, H. Maruyama, T. Suzuki, H. Ishida, M. Kojima, R. Glaser, *Cryst. Growth Des.*, 2014, **14**, 3692; (*b*) A. T. Gubaidullin, A. I. Samigullina, Z. A. Bredikhina, A. A. Bredikhin, *CrystEngComm*, 2014, **16**, 6716; (*c*) P. S. Carvalho, J. Ellena, D. S. Yufit, J. A. K. Howard, *Cryst. Growth Des.*, 2016, **16**, 3875; (*d*) I. Bouamaied, E. C. Constable, C. E. Housecroft, M. Neuburger, J. A. Zampese, *Dalton Trans.*, 2012, **41**, 10276; (*e*) R. Laubenstein, M. D. Serb, U. Englert, G. Raabe, T. Braun, B. Braun, *Chem. Commun.*, 2016, **52**, 1214; (*f*) U. B. Rao Khandavilli, M. Lusi, B. R. Bhogala, A. R. Maguire, M. Stein, S. E. Lawrence, *Chem. Commun.*, 2016, **52**, 8309; (*g*) A. Steinberg, I. Ergaz, R. A. Toscano, R. Glaser, *Cryst. Growth Des.*, 2011, **11**, 1262; (*h*) R. Bishop, M. L. Scudder, *Cryst. Growth Des.*, 2009, **9**, 2890; (*i*) I. Bernal, R. A. Lalancette, *C. R. Chim.*, 2015, **18**, 929.

15 (*a*) K. Murashima, S. Karasawa, K. Yoza, Y. Inagaki, N. Koga, *Dalton Trans*, 2016, **45**, 7067; (*b*) F. Pointillart, Y. Le Gal, S. Golhen, O. Cador, L. Ouahab, *Chem. Eur. J.*, 2011, **17**, 10397; (*c*) T. Han, W. Shi, X. P. Zhang, L. L. Li, P. Cheng, *Inorg. Chem.*, 2012, **51**, 13009; (*d*) W. H. Zhu, S. Li, C. Gao, X. Xiong, Y. Zhang, L. Liu, A. K. Powell, S. Gao, *Dalton Trans.*, 2016, **45**, 4614; (*e*) Q. Chen, J. Li, Y. S. Meng, H. L. Sun, Y. Q. Zhang, J. L. Sun, S. Gao, *Inorg. Chem.*, 2016, **55**, 7980; (*f*) J. Yang, F. Ma, X. B. Deng, H. L. Sun, Y. Q. Zhang, *CrystEngComm*, 2017, **19**, 4025.

16 G. M. Sheldrick, *Acta Cryst. C*, 2015, **71**, 3.

17 L. C. Thompson, S. C. Kuo, *J. Less. Common. Met.*, 1989, **148**, 173.

18 (*a*) M. Pinsky, D. Avnir, *Inorg. Chem.*, 1998, **37**, 5575; (*b*) D. Casanova, J. Cirera, M. Llunell, P. Alemany, D. Avnir, S. Alvarez, *J. Am. Chem. Soc.*, 2004, **126**, 1755; (*c*) J. Cirera, E. Ruiz, S. Alvarez, *Chem. Eur. J.,* 2006, **12**, 3162.

19 Y. N. Guo, G. F. Xu, Y. Guo, J. Tang, *Dalton Trans.*, 2011, **40**, 9953.

20 (*a*) A. Singh, K. N. Shrivastava, *Phys. Status Solidi B*, 1979, **95**, 273; (*b*) K. N. Shrivastava, *Phys. Status Solidi B*, 1983, **117**, 437.

21 A. Zabala-Lekuona, J. Cepeda, I. Oyarzabal, A. Rodríguez-Diéguez, J. A. García, J. M. Seco, E. Colacio, *CrystEngComm*, 2017, **19**, 256.
22 (*a*) T. Hang, W. Zhang, H. Y. Ye, R. G. Xiong, *Chem*. *Soc*. *Rev*., 2011, **40**, 3577; (*b*) Z. Chen, Y. Shen, L. Li, H. Zou, X. Fu, Z. Liu, K. Wang, F. Liang, *Dalton Trans*., 2017, **46**, 15032.

